

PACS numbers: 42.82.Bq; 42.82.Et; 07.60.Ly
DOI: 10.1070/QE2013v043n12ABEH015300

Fabrication-tolerant integrated polarisation splitter based on cascaded Mach–Zehnder interferometers

A.Yu. Koshelev, A.Yu. Goltsov

Abstract. **We report a fabrication-tolerant polarisation splitter based on cascaded Mach–Zehnder interferometers. This configuration enables a factor of 2–3 increase (at the 20 dB level) in the tolerance to the phase difference in comparison with a single interferometer. As an example, we present numerical simulation of a splitter with a centre wavelength of 650 nm, based on a planar waveguide from Si_3N_4. The permissible channel waveguide width deviation from calculation results (20-dB extinction coefficient bandwidth) is ~8% (~30 nm) for the TE polarisation and ~30% (100 nm) for the TM polarisation.**

Keywords: *integrated optics, polarisation splitter, Mach–Zehnder interferometer, silicon nitride, beam propagation method (BPM).*

1. Introduction

One limitation of integrated optical devices is their polarisation sensitivity, which leads to ambiguity in the reconstruction of emission spectra, e.g. in demultiplexers and on-chip spectrometers [1, 2]. One way to overcome the polarisation sensitivity is to produce separate integrated optical circuits for each polarisation [3]. Central to this approach are integrated optical polarisation splitters.

Various structures are used to fabricate polarisation splitters: multimode interference devices [4], directional couplers [5, 6], Mach–Zehnder interferometers (MZIs) [7], photonic crystals [8] and others. Such devices are typically intended for applications in silicon photonics and operate at a wavelength of 1.5 μm. One of their drawbacks is their sensitivity to fabrication tolerances. There is considerable interest in the ability to use such devices in the visible range, which means, from the practical point of view, a transition to lower contrast (smaller index difference) waveguides. This leads to a decrease in birefringence and makes polarisations even more difficult to separate. As a result, the devices become even more sensitive to fabrication tolerances, which causes a need to induce birefringence through additional etching [9] or metal deposition [10]. The purpose of this work was to design a fabrication-tolerant polarisation splitter for visible light using a moderate index contrast (silicon nitride, $n_{core} = 2$, $n_{clad} = 1.45$) planar waveguide and structures with one etching depth, without additional structures on the surface of the waveguide layer.

The device was built around an MZI-based polarisation splitter [7]. To reduce its sensitivity to fabrication tolerances, several such interferometers were cascaded using directional couplers. This approach was employed previously to create fabrication-tolerant optical couplers [11] and interleavers [12].

2. Polarisation splitter design

Figure 1 shows a schematic of a standard MZI-based polarisation splitter. After entering the polarisation splitter through one of the ports, the beam is divided into two equal parts by a directional coupler, which is often replaced by a multimode interference structure. The channel waveguides in the MZI arms are identical in length but differ in width. Note that such a device offers enhanced birefringence because the effective refractive indices of the TE and TM waveguide modes depend differently on channel waveguide width. The parameters of the waveguides are adjusted so that the difference in phase shift between the interferometer arms is 2π for the TM polarisation and π for the TE polarisation. Thus, the TM-polarised light will be coupled into the crossover waveguide, whereas the TE polarisation will remain in the straight-through waveguide. Such a configuration allows one to obtain large extinction coefficients, but it is very sensitive to fabrication tolerances, which influence the difference in phase shift between the interferometer arms.

Dai et al. [13] recently proposed using heaters to compensate for changes in the difference in phase shift between the interferometer arms. This approach, however, adds significant complexity to the design of the instrument. To reduce the sensitivity of polarisation splitters, we propose using a cascade of four interferometers. Interferometers and directional

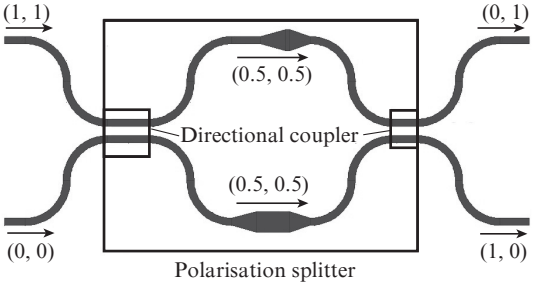

Figure 1. Schematic of a standard MZI-based polarisation splitter. The numbers in brackets specify the fraction of light in the corresponding waveguide for the TM and TE polarisations.

A.Yu. Koshelev, A.Yu. Goltsov Moscow Institute of Physics and Technology (State University), Institutskii per. 9, 141700 Dolgoprudnyi, Moscow region, Russia;
e-mail: koshelev@phystech.edu, goltsovalexander@gmail.com

Received 28 August 2013; revision received 9 October 2013
Kvantovaya Elektronika **43** (12) 1154–1158 (2013)
Translated by O.M. Tsarev

couplers will be utilised with appropriate phase differences and splitting ratios. Assume first that the splitting ratio is the same for the two polarisations, whereas the difference in phase shift is polarisation-dependent and can take arbitrary values. (Actually, the splitting ratio for the TE polarisation is smaller than that for the TM, but, as shown below, this only increases the stability of the system.) Our purpose is to find such splitting ratios and differences in phase shift at which polarisation splitting will be least sensitive to a ~1 rad detuning of the difference in phase shift. To simplify the optimisation procedure, we used two types of directional couplers, with splitting ratios $K_{1,2} = \sin^2(2\pi\theta_{1,2})$, where $\theta_{1,2}$ are the angular coupling coefficients, and identical interferometers with a difference in phase shift φ. The interferometers were placed antisymmetrically. A block diagram of the instrument is presented in Fig. 2.

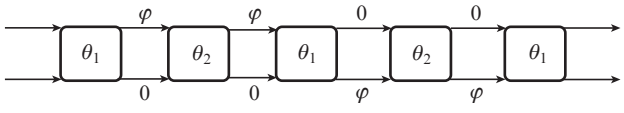

Figure 2. Block diagram of the MZI. The directional couplers are represented by rectangles, where θ_1 and θ_2 are the angular coupling coefficients. The arrows represent the interferometer arms; φ and 0 are phase differences.

The transfer functions of a directional coupler and interferometer have the form

$$\begin{pmatrix} E_0^{\text{out}} \\ E_1^{\text{out}} \end{pmatrix} = \begin{pmatrix} \cos\theta & -i\sin\theta \\ -i\sin\theta & \cos\theta \end{pmatrix} \begin{pmatrix} E_0^{\text{in}} \\ E_1^{\text{in}} \end{pmatrix} = A(\theta) \begin{pmatrix} E_0^{\text{in}} \\ E_1^{\text{in}} \end{pmatrix},$$

$$\begin{pmatrix} E_0^{\text{out}} \\ E_1^{\text{out}} \end{pmatrix} = \begin{pmatrix} e^{-i\varphi} & 0 \\ 0 & 1 \end{pmatrix} \begin{pmatrix} E_0^{\text{in}} \\ E_1^{\text{in}} \end{pmatrix} = B(\varphi) \begin{pmatrix} E_0^{\text{in}} \\ E_1^{\text{in}} \end{pmatrix},$$

where $E_{0,1}^{\text{in}}$ and $E_{0,1}^{\text{out}}$ are the field amplitudes in the zeroth and first channels at the input and output, respectively, and θ is the angular coupling coefficient.

Let all of the input radiation be in the zeroth channel. The transfer function of the instrument is then given by

$$\begin{pmatrix} E_0^{\text{out}} \\ E_1^{\text{out}} \end{pmatrix} = A(\theta_1)B(-\varphi)A(\theta_2)B(-\varphi)A(\theta_1)B(\varphi)$$

$$\times A(\theta_2)B(\varphi)A(\theta_1)\begin{pmatrix} 1 \\ 0 \end{pmatrix}. \qquad (1)$$

The optical power in the straight-through waveguide is $P_0 = |E_0^{\text{out}}|^2$, and that in the crossover waveguide is then $P_1 = 1 - P_0$.

To analyse the output signals as functions of the difference in phase shift in order to find flat peaks, we used the parameters $\theta_1 = 0.29$ rad and $\theta_2 = 0.4$ rad. The obtained power in the crossover waveguide as a function of the difference in phase shift is displayed in Fig. 3. Also presented for comparison are $P(\varphi)$ data for a standard polarisation splitter. It is seen that, in the region of the peaks, where complete polarisation splitting occurs, the transfer function varies more gradually in the case of the cascaded interferometers.

Figure 4 shows the extinction coefficient as a function of the detuning of the difference in phase shift between the interferometer arms (the nominal phase shift in the straight-through waveguide is π and that in the crossover waveguide is zero). It is seen that, in the case of the cascade of interferometers, the 20-dB bandwidth is ±0.39 rad for the TE polarisation and ±0.61 rad for the TM polarisation. The allowed detuning range for the standard interferometer is ±0.20 rad. Thus, the use of a cascade of interferometers enabled a factor of 2–3 increase in fabrication tolerances.

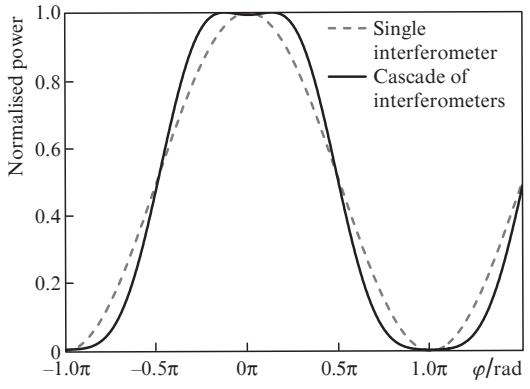

Figure 3. Optical power in the crossover waveguide as a function of the difference in phase shift between the MZI arms for a single interferometer and a cascade of interferometers.

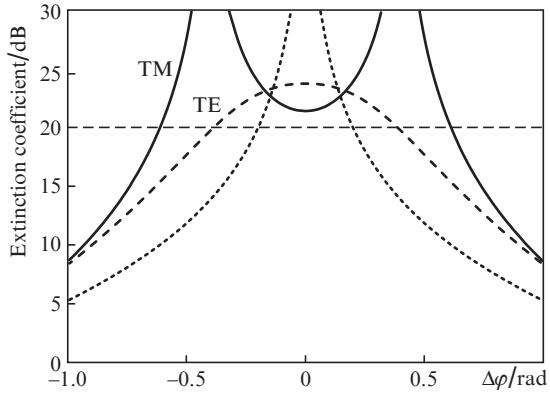

Figure 4. Extinction coefficient as a function of the detuning of the difference in phase shift between the interferometer arms. The permissible detuning (20-dB extinction coefficient bandwidth) in the cascade of interferometers (solid and dashed lines) is ±0.39 rad for the TE polarisation and ±0.61 rad for the TM polarisation. The allowed detuning in the standard interferometer (dotted lines) is ±0.20 rad.

3. Numerical simulation and discussion

To illustrate our method, we performed numerical simulation of the proposed design of a polarisation splitter with a centre wavelength of 650 nm, based on a standard planar waveguide from Si_3N_4 ($n \sim 2$), with a 160-nm-thick waveguide layer. Channel waveguides were produced by etching over the entire thickness of the waveguide layer in order to avoid uncertainties related to errors in etching depth. The upper and lower cladding layers were of SiO_2 ($n \sim 1.45$). The effective refractive indices of modes were found using the beam propagation method (BPM). The calculation results are presented in Fig. 5.

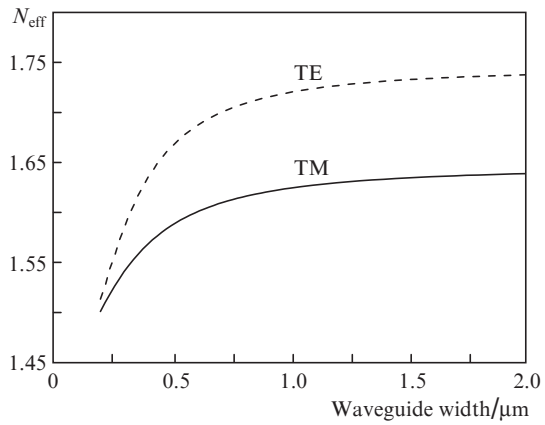

Figure 5. Effective refractive index as a function of channel waveguide width.

Taking into account the phase shift in the interferometer for the TE and TM polarisations, we have

$$n^{TE}(w_1)L_1 - n^{TE}(w_2)L_2 = \lambda/2,$$
$$n^{TM}(w_1)L_1 - n^{TM}(w_2)L_2 = 0, \quad (2)$$

where $w_{1,2}$ are the waveguide widths and $L_{1,2}$ are the waveguide lengths.

The solutions to this equation at various combinations of w_1 and w_2 are presented in Fig. 6. The major source of errors in the fabrication of channel waveguides is the deviation of their width from the nominal one. A characteristic change in the difference in phase shift was evaluated as the root mean square of its variation upon an increase and decrease in waveguide width by 10%. Based on practical considerations – sufficient waveguide widths, a small interferometer arm length and stability to width changes – we took $w_1 = 445$ nm, $w_2 = 370$ nm, $L_1 = 29.7$ μm and $L_2 = 30$ μm. Figure 7 shows the difference in phase shift as a function of waveguide width deviation.

The waveguide widths influence the splitting ratios of the directional couplers. In selecting the parameters d (separation between the waveguides) and l (coupling length) of the directional coupler at a given splitting ratio, smaller lengths are preferable because this increases the spectral range of the instrument. From the practical point of view, the effective coupling length is limited by the radii of input bent waveguides. To avoid bending losses, we took a radius of 60 μm. The parameters d and l also depend on waveguide width. For each d value, there is an optimal waveguide width at which the exchange coefficient is minimal. At this width, waveguide width deviations cause, to a first approximation, no changes in splitting ratio. Based on these considerations, we took the following parameters of the directional couplers: $d_1 = d_2 = 370$ nm, $l_1 = 0.13$ μm and $l_2 = 2.71$ μm at $w_1 = w_2 = 370$ nm. Figures 8 and 9 show the splitting ratios $K_{1,2} = \sin^2(\theta_{1,2})$ and extinction coefficient [found using Eqn (1)] as functions of waveguide width deviation.

Note that the fabrication-tolerant polarisation splitter in question is about four times as long as a conventional splitter.

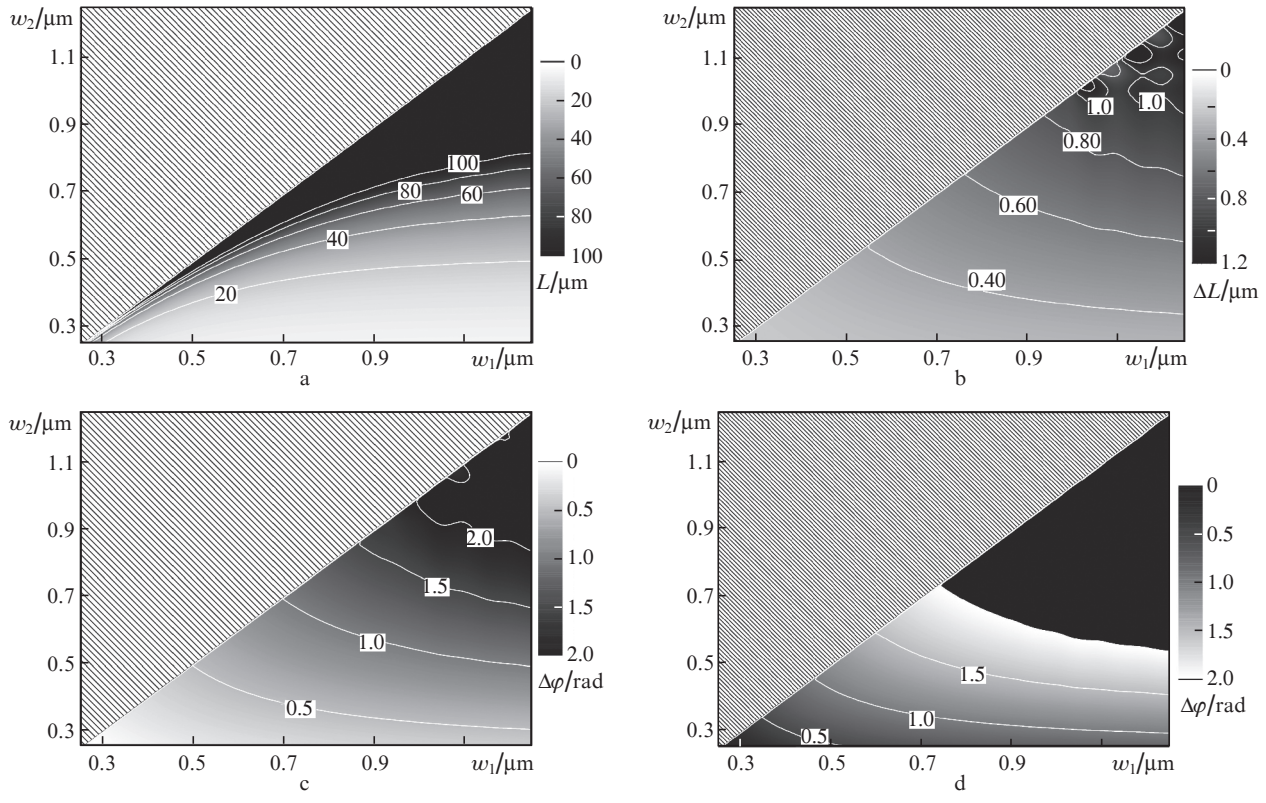

Figure 6. (a) Average interferometer arm length $L = (L_1 + L_2)/2$ and (b) difference between the arm lengths $\Delta L = (L_1 - L_2)/2$ as functions of waveguide widths w_1 and w_2 ; (c, d) characteristic change in the difference in phase shift between the interferometer arms upon a change in w_1 and w_2 by 10% for the TM and TE polarisations, respectively.

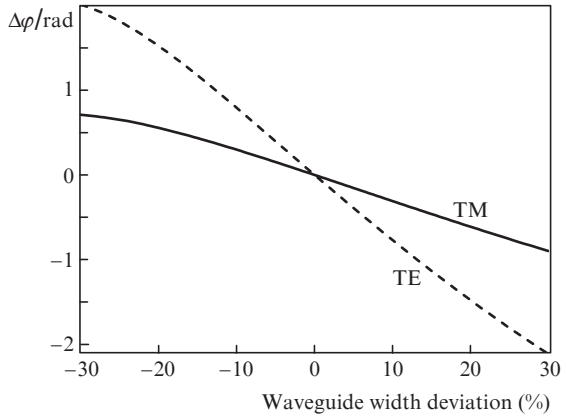

Figure 7. Phase difference between the interferometer arms as a function of waveguide width deviation.

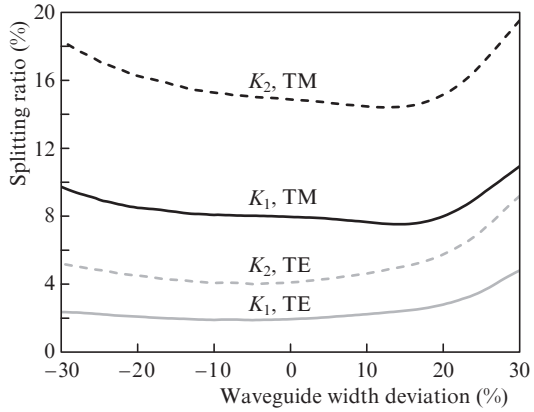

Figure 8. Splitting ratios of directional couplers as functions of waveguide width deviation for the TE and TM polarisations.

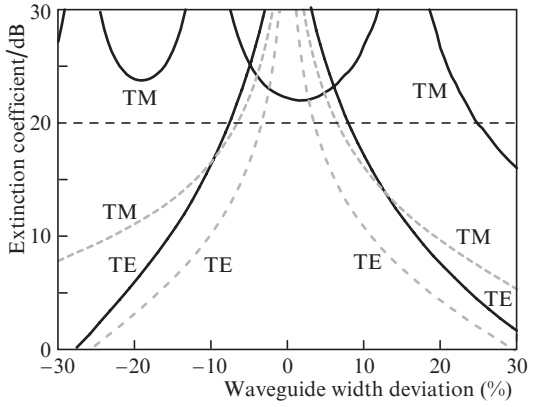

Figure 9. Extinction coefficient as a function of waveguide width deviation with allowance for the variation in the splitting ratio of the directional couplers. The permissible width deviation (20-dB extinction coefficient bandwidth) in the cascade of interferometers (solid lines) is ±7.6% for the TE polarisation and ∼±30% for the TM polarisation. The permissible width deviation in the standard interferometer (dashed lines) is ±3.3% for the TE polarisation and ±6.2% for the TM polarisation.

This may lead to an increase in losses. The losses in polarisation splitters can be divided into two groups: the loss in the channel waveguides (attenuation in the material and scattering by the roughness of the vertical wall) and that in the other components of the system. The loss in the channel waveguides depends on the fabrication quality and is typically in the range 0.5–1 dB cm^{-1} [14, 15], which leads to a low loss (under 0.1 dB) over the polariser length (∼700 μm). The loss in the components of the system is caused by the bent portions and adiabatic expansions of the waveguide. Since the waveguide width is assumed to vary uniformly (gradually within the structure being fabricated) with fabrication changes, the variation in the loss in the components of the system is primarily due to the deviation of the widths of the bent waveguides from the optimal one at a given bend radius. The calculated additional loss in the proposed configuration is presented in Fig. 10 for the TE and TM polarisations. It is seen that the additional loss is within 0.7 dB, which is quite acceptable. Clearly, the loss can be reduced by increasing the radius of curvature and length of adiabatic transitions.

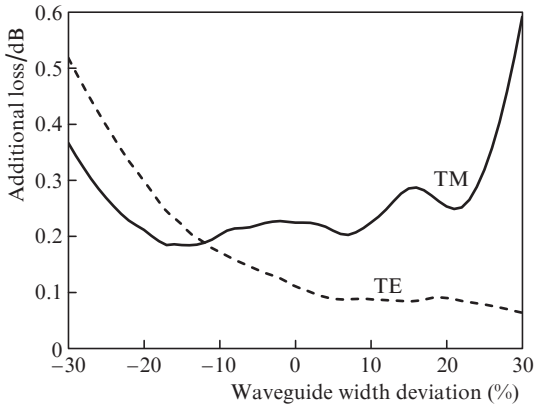

Figure 10. Additional loss in the proposed polarisation splitter configuration vs. waveguide width deviation for the TE and TM polarisations.

Figure 11 presents BPM simulation results for the structure under consideration. Note that, because it has nonzero light propagation angles, light propagation simulation would be generally expected to give less accurate results in comparison with Eqn (1).

It is worth pointing out that the assumption used in the numerical simulation that the predominant source of errors is a uniform variation in waveguide widths may be invalid in the case of a real fabrication process. Nevertheless, it follows from Fig. 4 that the use of a cascade of interferometers allows better results to be obtained regardless of the origin of deviations in the difference in phase shift between the interferometer arms.

4. Conclusions

We have described a fabrication-tolerant polarisation splitter based on cascaded Mach–Zehnder interferometers. This configuration enables an increase in the tolerance to the phase difference in the interferometer by a factor of 2 for the TE polarisation and by a factor of 3 for TM-polarised light in comparison with a single interferometer.

The use of this approach is exemplified by numerical simulation of a splitter with a centre wavelength of 650 nm, based on a planar waveguide from Si_3N_4. The permissible channel waveguide width deviation (20-dB extinction coefficient

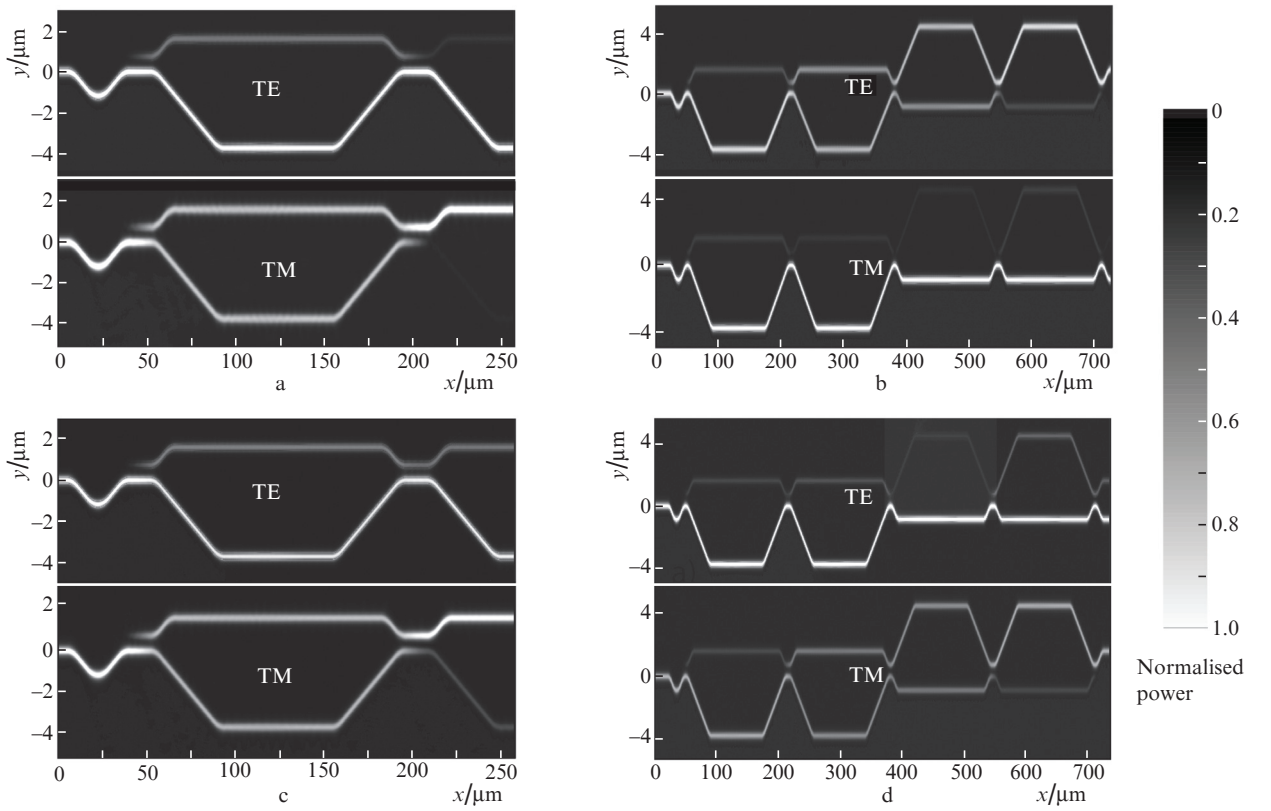

Figure 11. Simulation results for optical power P propagation along (a) a standard polarisation splitter with nominal parameters, (b) along a cascade of interferometers with nominal parameters and (c, d) along a standard polarisation splitter and a cascade of interferometers, respectively, with all the waveguide widths reduced by 20%.

bandwidth) is 7.6% (~30 nm) for the TE polarisation and ~30% (100 nm) for the TM polarisation.

The increase in the overall splitter length (to ~1 mm) relative to conventional splitters leads to an only slight increase in loss (by less than 1 dB).

The use of the proposed approach for simulating polarisation splitters simplifies the development of polarisation-insensitive devices based on moderate index contrast waveguides for the visible and near-IR spectral regions.

Acknowledgements. This work was supported by the Skolkovo Foundation (Grant No. 86).

References

1. Sherwood N., Nitkowski A., Preston K., Berkeley A., Schmidt B.S., Hajian A. *Conf. Advanced Photonics 2013*. OSA Techn. Dig.(online) (Opt. Soc. Am., 2013) paper IW4A.6.
2. Peroz C., Calo C., Goltsov A., Dhuey S., Koshelev A., Sasorov P., Ivonin I., Babin S., Cabrini S., Yankov V. *Opt. Lett*., **37**, 695 (2012).
3. Barwicz T., Watts M.R., Popovic P.A., Rakich P.T., Socci L., Kartner F.X., Ippen E.P., Smith H.I. *Nat. Photonics*, **1**, 57 (2007).
4. Hong J.M., Ryu H.H., Park S.R., Jeong J.W., Lee S.G., Lee E.-H., Park S.-G., Woo D., Kim S., O B.-H. *IEEE Photonics Technol. Lett*., **15**, 72 (2003).
5. Augustin L.M., van der Tol J.J.G.M., Hanfoug R., De Laat W.J.M., et al. *J. Lightwave Technol*., **25**, 740 (2007).
6. Dai D., Bowers J. *Opt. Express*, **19**, 18614 (2011).
7. Dai D., Wang Z., Peters J., Bowers J.E. *IEEE Photonics Technol. Lett*., **24**, 673 (2012).
8. Shi Y., Dai D., He S. *IEEE Photonics Technol. Lett*., **19** (11), 825 (2007).
9. Watts M.R., Haus H.A., Ippen E.P. *Opt. Lett*., **30**, 967 (2005).
10. Albrecht P., Hamacher M., Heidrich H., Hoffmann D., Nolting H., Weinert C.M. *IEEE Photonics Technol. Lett*., **2**, 114 (1990).
11. Chang S.-J., Liu K.-W. *Opt. Eng*., **51** (9), 094603 (2012).
12. Cherchi M. *J. Opt. Soc. Am. B*, **23**, 1752 (2006).
13. Dai D., Wang Z., Bowers J.E. *J. Lightwave Technol*., **29** (12), 1808 (2011).
14. Romero-Garcна S., Merget F., Zhong F., Finkelstein H., Witzens J. *Opt. Express*, **21**, 14036 (2013).
15. Gorin A., Jaouad A., Grondin E., Aimez V., Charette P. *Opt. Express*, **16**, 13509 (2008).